Available online at www.sciencedirect.com
ScienceDirect
Journal of Hazardous Materials 149 (2007) 666–674
Journal of Hazardous Materials
www.elsevier.com/locate/jhazmat

Mathematical modeling for the evaluation of zinc removal efficiency on clay sorbent

M. Sarkar [a,*], A.R. Sarkar [a], J.L. Goswami [b]

[a] *Department of Chemistry, University of Kalyani, Kalyani 741235, West Bengal, India*
[b] *WMD, NRG, Bhabha Atomic Research Centre, Mumbai 400085, India*

Received 6 December 2006; received in revised form 5 April 2007; accepted 9 April 2007
Available online 19 April 2007

Abstract

The adsorption characteristics of zinc ion from aqueous solution on the lateritic clay were investigated through batch and column mode of operation. The system variables were optimized to evaluate the maximum extent of zinc adsorption as well as for the purpose of modeling. A model equation correlating zinc adsorption with input concentration was described. The adsorption behavior can well be described by Freundlich isotherm model rather than Langmuir isotherm model. The favorable and spontaneous nature of adsorption was indicated from the thermodynamical parameters. The capacity was determined from isotherm parameters in batch mode and breakthrough parameters in column mode. The bed depth service time (BDST) model was utilized to predict column efficiency corresponding to different bed heights. Elution performance of retained zinc, using HNO_3 of definite composition, was examined from elution profile. Efficiency of the process was determined through repetitive operation cycles of retention and elution. Effectiveness of the process was judged through estimation of efficiency versus the cost of operation.

Keywords: Adsorption; Zinc; Clay; Optimization; Efficiency

1. Introduction

Metal ions are probably the oldest toxins known to mankind and since they are not subjected to biodegradation and for all practical purposes they have infinite residence time in different environment compartments. However, the degree of toxicity varies greatly depending on the metal itself and its mode of action on the specific organism [1]. The introduction of heavy metals in water is of serious concern as they not only change the natural quality but also pose threat to aquatic lives. The ever increasing demand of water of high quality, moreover, has caused considerable attention to be focused towards the recovery and reuse of waste water and, therefore, the removal and recovery of metal ion from industrial effluent is of great significance.

The main industrial use of zinc is for manufacturing of zinc white, several useful alloys such as brass, German silver, delta metal and as the anode material in galvanic cells. Lithographic plates are also made of zinc. Zinc has a secondary drinking water standard of 5.0 mg dm^{-3} principally because of its bitter metallic taste [2]. The average human body contains about 2 g of zinc, which is essential for the normal activity of DNA polymerization and for protein synthesis. Zinc toxicity from excessive ingestion is uncommon but gastrointestinal distress and diarrhea has been known following ingestion of beverages standing in galvanized cans or from use of galvanized utensils. With regard to industrial exposure, zinc fume fever resulting from inhalation of freshly formed fumes presents the most significant effect. Edema of the lungs from fumes of zinc chloride ($ZnCl_2$ smoke) is sometimes fatal. Soluble and astringent acid salts, such as $ZnSO_4$ in large doses (about 10 g), have caused internal organ damage and death [1]. The plants grown on zinc enriched soil also show various abnormalities and disorders like reduction of growth, inhibition of photosynthesis and respiration together with interruption of metabolism linked to the transport processes. Removal and recovery of zinc is necessary in the context of minimization of toxicity and improvement of analytical determination via preconcentration.

Liquid–liquid extraction, one of the useful technologies for the removal of metal ions from aqueous samples involves large volume of solvent, tedious process and large through output.

* Corresponding author. Tel.: +91 33 25823883; fax: +91 33 25828282.
E-mail address: mitali_ku@yahoo.com (M. Sarkar).

0304-3894/$ – see front matter © 2007 Elsevier B.V. All rights reserved.
doi:10.1016/j.jhazmat.2007.04.027

Solid phase extraction or adsorption, on the other hand, is gaining popularity, primarily because of its simplicity and availability of a wide variety of adsorbent viz. natural, synthetic as well as the biomaterial. Natural adsorbents like soil, clay and mineral [3–6] has the advantage of easy availability and low cost. Similarly, use of waste materials [7–10] has benefit of low cost and overcoming disposal problem via utilization. Synthetic adsorbents like activated carbon [11], ion exchange material [12], chelate impregnated silica [13,14] and polymer matrices [15,16] are popular due to high removal capacity. A number of reports on the adsorption of Zn(II) on the sludge [17,18] and bioadsorbents [19–21] are available. Recently, zinc(II) removal from water with purified carbon nanotubes [22], TiO_2 (110)–electrolyte interface [23] and manganese nodule leached residues [24] is reported. As the recent progress in chemical analysis of trace metal ions is mainly connected with the evaluation and improvement of various separation and trace concentration methods, the present study reports the adsorption behavior of zinc(II) from aqueous solution on some naturally occurring lateritic clay.

2. Experimental

2.1. Materials

All the chemicals were of analytical-reagent grade. A stock solution (1000 mg dm^{-3}) of Zn(II) was prepared by dissolving zinc sulphate (purity 99%; E. Merck, India) in doubly distilled water. The laterite soil was collected from Bankura District, West Bengal, India. It was washed several times to remove the earthy matter and finally with distilled water. It was then air dried and ground manually to obtain desired particle sizes using scientific molecular sieves (Geologists' Syndicate, Calcutta, India). X-ray diffraction (XRD) data was obtained by a diffractometer (Rigaku Miniflex ME 200CY2, Japan) with powdered sample using Cu Kα radiation. The as-received laterite sample, without further grinding and size classification, is subjected to morphological characterization through scanning electron microscopy (SEM) analysis with an Environmental Scanning Electron Microscope, Philips, (model ESEM XL-30, Netherlands) at 25 kV. The zero point charge of laterite was determined potentiometrically using an Orion pH/mV meter (model no. 701) with glass (Fischer 13-639-3) and calomel (Fischer 13-639-52) electrode. An atomic absorption spectrophotometer (Varian AA1407, USA) was used for determination of metal ions. The characteristic features are lamp current 5.0 mA, wavelength 213.9 nm, slit width 1.0 mm using an air-acetylene flame with the observation at 10 cm above the burner. The quality assurance and standardization of determination was made with standard metal ion solution (Certipure®; E. Merck, Germany).

2.2. Adsorption studies

Batch experiment was performed to obtain rate, equilibrium and isotherm data. The flask containing 20 cm^3 of Zn(II) solution (20–200 mg dm^{-3}) at the required pH was shaken with laterite (1.0 g) in a mechanical shaker until the equilibrium is attained. The amount of Zn(II) in the supernatant was determined by atomic absorption spectroscopic measurement [25]. The amount of Zn(II) adsorbed (q_e) per gram of laterite (mg g^{-1}) was determined by the equation:

$$q_e = \frac{X - Y}{Z} \quad (1)$$

where X is the amount of Zn(II) added (mg), Y the amount of Zn(II) remained in supernatant (mg) and Z is the mass of laterite (g).

Column experiment was performed for retention and subsequent elution. The column (0.6 cm × 60.0 cm) was packed with laterite of uniform size following the procedure of Fornwalt and Hutchins [26]. The mass of the laterite required was 0.87 g cm^{-1} of the column bed with packed bed density of 1.03 g cm^{-3} and void volume of 1.61 cm^3. Zn(II) solution at a definite pH (between 2.0 and 8.0) was percolated at a uniform flow rate (controlled by a flow controller) through the column. The process was optimized for the feed Zn(II) concentration, flow rate and height of laterite column. The effluent was collected from the column end at regular interval of time and Zn(II) concentration was determined. After washing the column with de-ionized water, an eluting solution (HNO_3) of definite composition was passed through at uniform flow rate. The metal ion concentration in the eluate, after diluting to the desired volume, was determined by AAS.

3. Results and discussion

3.1. Characterization of laterite

Laterite sample was characterized through physico-chemical analysis together with SEM image (Fig. 1) and XRD pattern (Fig. 2) analysis. The chemical composition of laterite is described elsewhere [27]. SEM has identified a morphological class of spherical particles containing encapsulated smaller spheres [28]. Plerosphere formation here is truly the result of encapsulation during particle formation rather than filling of a ruptured cenosphere. Subsequent examination of the etched particles indicated the presence of numerous smaller particles within the plerospheres. XRD pattern indicates the presence of crystalline iron oxides such as goethite, hematite, lepidocrocite as well as amorphous iron oxides together with α-quartz and γ-alumina. The zero point charge (pH_{ZPC}) determined by potentiometric titration of laterite sample in presence of electrolyte is found to be 3.08.

3.2. Optimization of operational variables during batch study

The adsorption of Zn(II) on laterite is dependent on both the initial Zn(II) concentration and the agitation time. The effect of agitation time on adsorption of Zn(II) at different initial concentrations is presented in Fig. 3. It is observed that at each concentration, there is an increase in the amount adsorbed (mg g^{-1}) by increasing the agitation time. This is due to the availability of large vacant adsorbent sites as well as a high

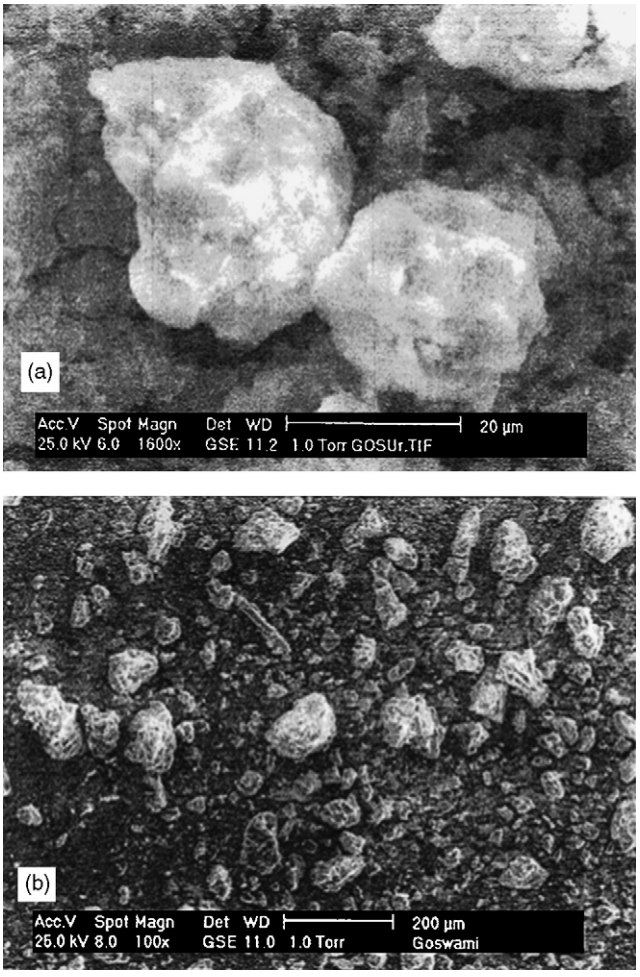

Fig. 1. Scanning electron micrographs for laterite. The bar indicates (a) 20 μm and (b) 200 μm.

concentration gradient between the solution and the solid phase [29]. The extent of Zn(II) uptake gradually slows down that ultimately reaches a maxima indicated by a flat plateau. The time (80 min) corresponding to the maximum adsorption is considered as the equilibrium adsorption time. The adsorption profiles for different concentrations show similar shape, only differing in the extent of adsorption. With the increase in Zn(II) concentration from 20 to 100 mg dm^{-3} the percent of adsorption decreases from 71 to 57%. The adsorption percent (p) decreases

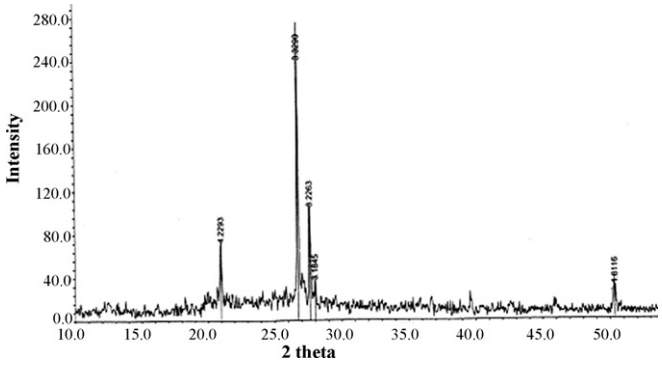

Fig. 2. XRD pattern of laterite.

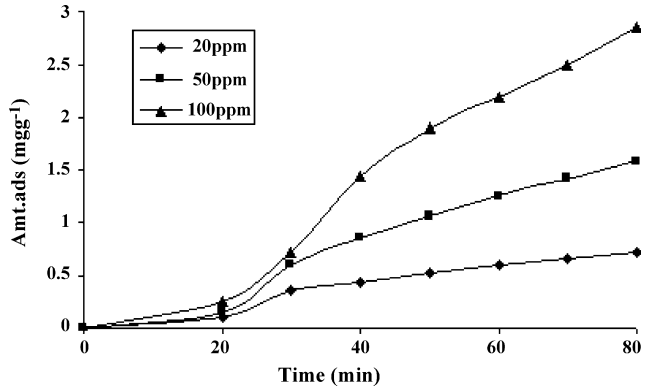

Fig. 3. The influences of agitation time and concentration of adsorbate on adsorption of zinc(II) on laterite in aqueous solutions at 293 K.

exponentially with increased Zn(II) concentration (C_0) and can be expressed as:

$$p = 106.7\, C_0^{-0.155} \quad (2)$$

Such model equation can be used to predict extent of Zn(II) removal at the solution condition of pH and temperature. Singh et al. [30] made similar type of correlation for dye adsorption on fly ash.

The effect of agitation speed on the extent of Zn(II) adsorption was investigated with variation of agitation speed from 100 to 400 rpm under equilibrium time and initial solute concentration (20 mg dm^{-3}). It is observed that with increase in agitation speed, adsorption increases from 41 to 71%. It may be thought that as the speed increases resistance to mass transfer from bulk to the adsorbent phase decreases resulting in increased adsorption rate [29].

Adsorption experiment performed with laterite of three different particle sizes (+1.0 to −0.8, +0.8 to −0.5 and +0.5 to −0.3 mm) at the selected equilibrium condition indicates that adsorption increases from 27 to 71% as the particle size decreases. With smaller particles, as the surface area increases, the solute finds more accessible sites for adsorption [29]. Although, with even the finer particles increased adsorption is expected, it sometimes creates operational complications, e.g. separation of finer laterite particle during filtration in batch operation and chocking of laterite bed during column operation.

The laterite dose was varied from 0.2 to 1.2 g per 50 cm^3 under equilibrium agitation time and initial solute concentration (20 mg dm^{-3}). It is observed that as the dose of laterite increases Zn(II) adsorption increases from 31 to 71% and reaches the maximum value corresponding to a dose of 1.0 g.

The effect of temperature on the extent of Zn(II) adsorption was investigated in the solution temperature range from 293 to 313 K at equilibrium. It is found that the percent of adsorption increases from 66 to 82% corresponding to an initial zinc concentration of 100 mg dm^{-3} (Fig. 4).

The adsorption pattern of Zn(II) on laterite with change in pH is presented in Fig. 5. The adsorption is found to be influenced by solution pH, as surface charge of laterite is governed by pH. The surface charge is assessed by the zero point charge (pH_{ZPC}) or the isoelectric point (IEP). pH_{ZPC} and IEP are the

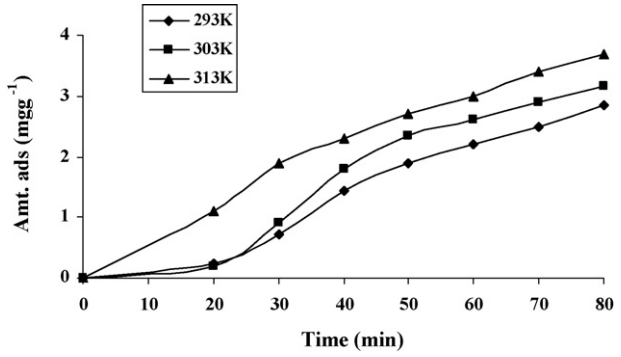

Fig. 4. The influences of agitation time and temperature of adsorbate on adsorption of zinc(II) on laterite in aqueous solutions at 100 ppm.

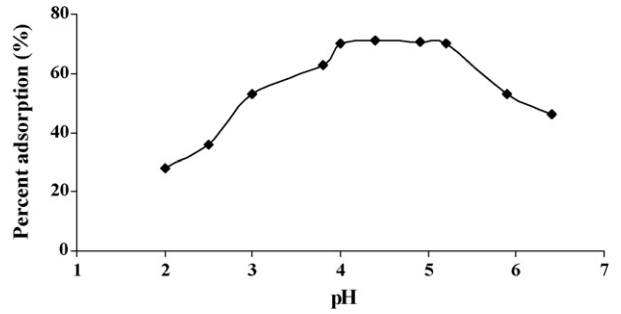

Fig. 5. The influences of pH on adsorption of zinc(II) on laterite in aqueous solutions at 20 ppm and 293 K.

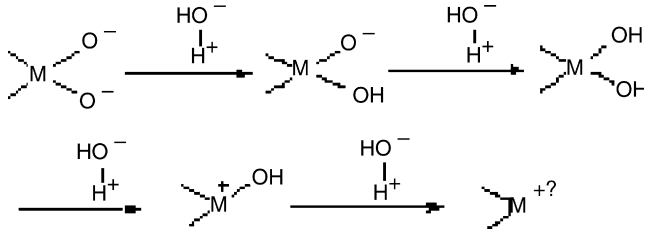

Scheme 1. pH dependent surface charge on laterite.

same if background electrolyte does not adsorb on the surface, as in case with laterite. The metal oxides present in laterite form aquo complexes with water and develop charged surface through amphoteric dissociation [31]. It is evident from Scheme 1 that at $pH < pH_{ZPC}$, the surface charge is positive, at $pH = pH_{ZPC}$, the surface charge is neutral and at $pH > pH_{ZPC}$, the surface charge is negative [32].

Thus, at lower pH (below pH_{ZPC}), as more of the surface sites are positively charged, adsorption of Zn(II) ion is inhibited by electrostatic repulsion. Zn(II) adsorption is found to be enhanced by increasing pH. An increase in Zn(II) adsorption is observed from 28 to 70% for increase in pH from 2.0 to 4.0.

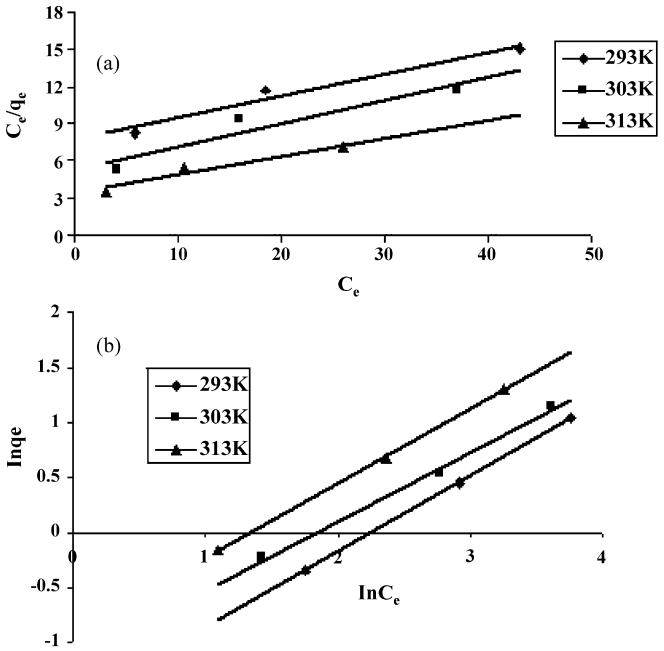

Fig. 6. (a) Langmuir and (b) Freundlich adsorption models applied for interaction of zinc(II) in aqueous solution on laterite.

Higher adsorption is found to occur in the pH region 4.0–5.2. The extent of Zn(II) adsorption decreases significantly beyond a pH 5.2.

3.3. Mathematical modeling of the adsorption isotherm

Several equilibrium models have been developed to describe adsorption isotherm relationships that play a functional role in predictive modeling procedure for analysis and design of an adsorption system [33]. The Langmuir and Freundlich isotherm are used most frequently to describe the adsorption data. The basic assumptions underlying Langmuir model describes the ideal localized monolayer formation and is generally expressed in linear form as:

$$\frac{C_e}{q_e} = \frac{1}{Qb} + \frac{C_e}{Q} \quad (3)$$

where C_e is the equilibrium Zn(II) concentration (mg dm^{-3}), q_e the equilibrium amount of Zn(II) on laterite (mg g^{-1}) and Q (mg g^{-1}) and b (dm^3 mg^{-1}) are the Langmuir isotherm constants related to the capacity and the energy, respectively. A plot of C_e/q_e against C_e (Fig. 6a) should yield a straight line with Q and b obtained from the intercept and the slope, respectively (Table 1).

Table 1
Evaluation of equilibrium and isotherm parameters for interaction of zinc(II) in aqueous solution on laterite

Temperature (K)	Q (mg g^{-1})	b.10^2 (dm^3 mg^{-1})	(R^2)	r			K_f (dm^3 g^{-1})	1/n	(R^2)
				20 (mg dm^{-3})	50 (mg dm^{-3})	100 (mg dm^{-3})			
293	5.60	2.25	0.9520	0.681	0.461	0.299	2.07	0.696	0.9998
303	5.37	3.53	0.9026	0.586	0.362	0.221	3.19	0.629	0.9952
313	6.87	4.29	0.9493	0.583	0.317	0.189	2.49	0.680	0.9998

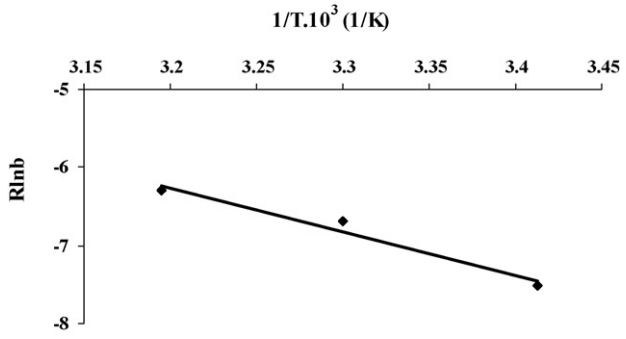

Fig. 7. Plot of van't Hoff curve.

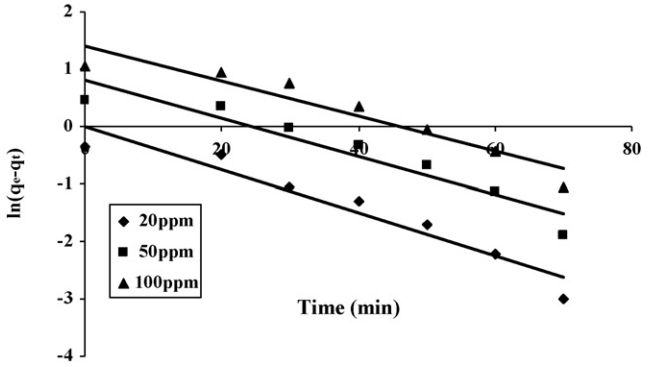

Fig. 8. Plot of Lagergren curves.

The Freundlich isotherm model, on the other hand, is assumed to be associated with heterogeneous sites and can be expressed in linear form as:

$$\ln q_e = \ln K_f + \left(\frac{1}{n}\right) \ln C_e \quad (4)$$

where K_f (mg g^{-1}) and $1/n$ signify capacity and the intensity, respectively. The intensity value less than 1 indicates the favorable situation (Table 1). A plot of ln q_e against ln C_e should yield a straight line with slope $1/n$ and intercept ln K_f (Fig. 6b).

The best isotherm equation to use in a particular instance is the one that better fits the experimental data. As indicated from the regression coefficient values (R^2) Freundlich model sufficiently describes the Zn(II)-laterite interaction. The isotherm criteria may further be described by a dimensionless quantity 'r', the constant separation factor [34], defined as:

$$r = \frac{1}{1 + bC_0} \quad (5)$$

where C_0 is the initial concentration and b is the Langmuir isotherm constant. The feasibility criteria of the process can be judged indicating unfavorable ($r > 1$), irreversible ($r = 0$), favorable ($0 < r < 1$) or linear ($r = 1$) pattern. The calculated 'r' values (between 0.189 and 0.681) in the studied concentration range indicate favorable case of adsorption at the selected operational conditions.

3.4. Evaluation of thermodynamic parameters

In order to study the feasibility of the process, thermodynamic parameters viz. ΔG, ΔH and ΔS of the process are calculated following the equations [35]:

$$\Delta G = -RT \ln b \quad (6)$$

$$R \ln b = \frac{-\Delta H}{T} + \Delta S \quad (7)$$

The negative value of ΔG (9.10 kJ mol^{-1} at 293 K) indicates that the adsorption process is favorable and spontaneous. ΔH and ΔS are obtained from slope and intercept, respectively (Fig. 7), from the van't Hoff plot (R ln b against $1/T$). The positive values of ΔH (23.19 J mol^{-1}) and ΔS (48.22 J mol^{-1} K^{-1}) denote that the process is endothermic and random in nature. The high regression value indicates the validity of the van't Hoff equation. The endothermic nature may also be predicted from increased adsorption with increased temperature.

3.5. Kinetics and rate parameters

The kinetic feasibility of Zn(II)-laterite interaction is indicated by the shorter (<30 min) $t_{1/2}$ (the time required for 50% adsorption) value. In order to find out the applicability of rate law kinetic data was fitted to a pseudo first order rate expression, i.e. the Lagergren [36] rate equation expressed as:

$$\ln(q_e - q_t) = \ln q_e - K_1 t \quad (8)$$

where q_e and q_t are the amount of Zn(II) (mg g^{-1}) on laterite at equilibrium and at time t, respectively, K_1 is the first order rate constant. A plot of $\ln(q_e - q_t)$ against time (t) should yield a straight line (Fig. 8) with K_1 obtained from the slope.

The data may be fitted to the pseudo second order expression expressed as:

$$\frac{t}{q_t} = \left(\frac{1}{K_2}\right)\left(\frac{1}{q_e^2}\right) + \frac{t}{q_e} \quad (9)$$

applying the boundary conditions of $t = 0$–t and $q_t = 0$–q_t. A plot of t/q_t against t should yield a straight line with K_2, the second order rate constant, and is obtained from the intercept.

The applicability of a particular rate expression was evaluated from the goodness of data fit and regression coefficient value. In the present situation, the Lagergren first order equation gives a higher regression value compared to the second order equation showing adherence to the pseudo first order rate law (Table 2). However, adsorption, being a complex phenomenon, generally follows a pathway comprising of a combination of the surface and the pore diffusion. The extent of a particular diffusion to the

Table 2
Evaluation of kinetic parameters and regression coefficients for interaction of zinc(II) in aqueous solution on laterite

Temperature (K)	K_1	R^2	K_2	R^2	K_d
293	0.0307	0.9011	0.0668	0.4225	0.3518
303	0.0372	0.8984	0.0354	0.3434	0.3704
313	0.0339	0.9369	0.0722	0.8230	0.4055

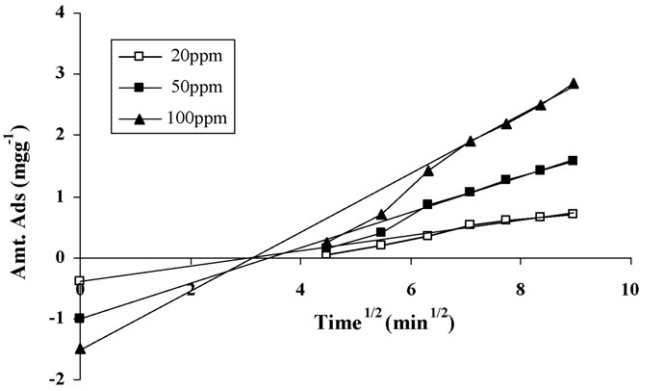

Fig. 9. Plot of Weber Morris curves.

total process may be estimated by a plot following Weber and Morris equation [37] expressed as:

$$q_t = K_d\sqrt{t} \quad (10)$$

where K_d, the rate constant of pore diffusion, is obtained from the slope of the linear portion of the plot q_t versus $\sqrt{t}$. The Weber and Morris plot (Fig. 9) reveals an initial curved portion (indicative of boundary layer effect, i.e. surface adherence) followed by a linear portion (indicative of intraparticle or pore diffusion). The slope of the linear portion yields K_d, while the intercept of the plot signifies the extent of boundary layer effect. The larger the intercept the greater is the contribution to the surface adherence [38] in the rate limiting step. It is found that K_d value increases with increased temperature (Table 2).The activation energy (E) of the pore diffusion is calculated [31] from the linear plot of ln K_d versus $1/T$ following Arrhenius equation:

$$\ln K_d = \ln A - \frac{E}{RT} \quad (11)$$

The goodness of the data fit is indicated by the high regression coefficient ($R^2 = 0.9685$) value of the Arrhenius plot (Fig. 10) and the E value is found to be 5.36 J mol^{-1}.

3.6. Optimization of operational parameters during column study

The operation and performance of a column is known to be influenced by several operational parameters viz. concentration

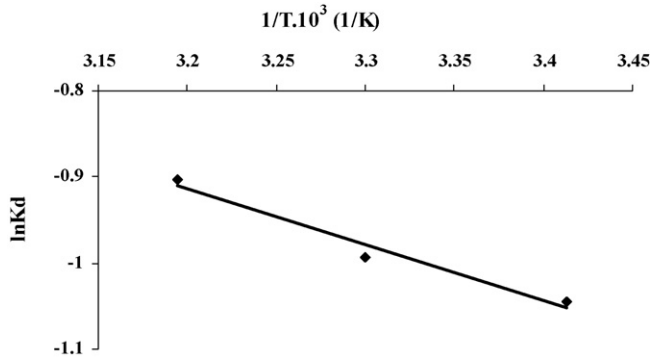

Fig. 10. Plot of Arrhenius curve.

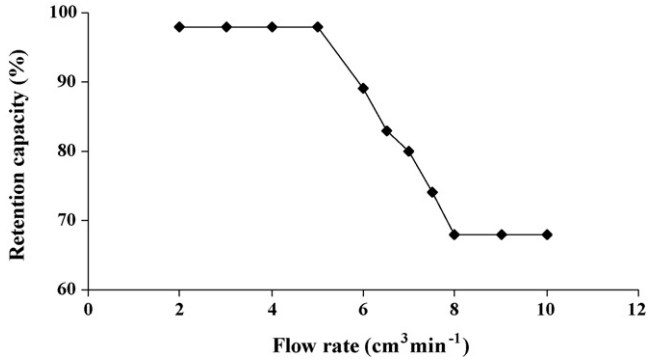

Fig. 11. Effect of flow rate on retention capacity of zinc(II) in aqueous solution.

and flow rate of the feed solution as well as column bed height. Optimization of such variables is essential to evaluate the column performance. The flow rate for the Zn(II) solution through the column was varied up to 10.0 cm^3 min^{-1} for a fixed Zn(II) concentration (100 mg dm^{-3}) and laterite bed height (20 cm). It is found that up to a flow rate 5.0 cm^3 min^{-1} column retention capacity remains unchanged and decreased thereafter (Fig. 11). Zn(II) retention on laterite packed column was investigated with different Zn(II) concentrations viz., 20, 50 and 100 mg dm^{-3}. The characteristic shape and position of breakthrough curve (BTC) on the volume axis for a fixed laterite bed length of 20 cm is presented in Fig. 12a. The parameters like breakthrough volume and time (V_b, t_b), exhaustion volume and time (V_x, t_x) are presented in Table 3. As the feed Zn(II) concentration increases, the breakthrough time decreases. Sharp BTC is obtained for high Zn(II) concentration, while the BTC corresponding to low Zn(II) concentration flattens. The effect of bed height on Zn(II)

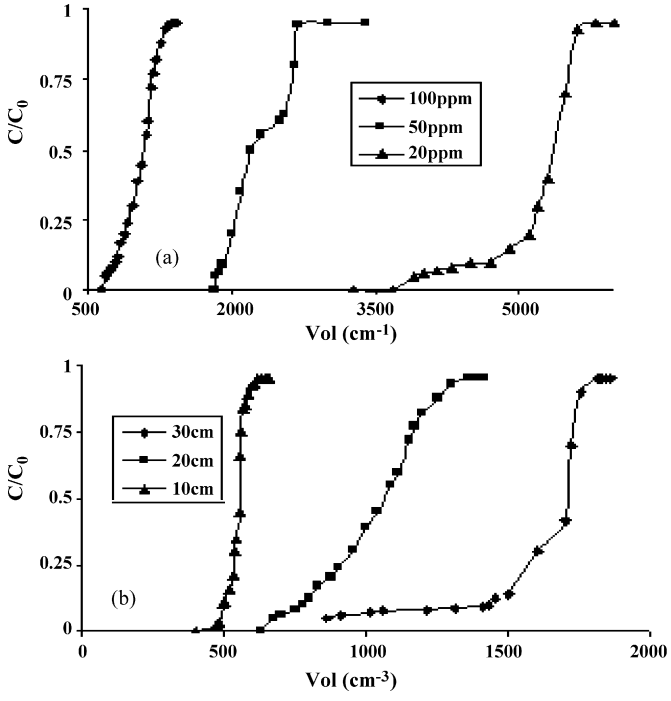

Fig. 12. Plot of BTC (a) at different concentrations and at a fixed bed height of 20 cm and (b) at different bed heights and fixed zinc(II) concentration of 100 ppm.

Table 3
Evaluation of characteristic parameters for retention of zinc(II) from aqueous solution on fixed bed laterite column

C_0 (mg dm^{-3})	D (cm)	V_x (cm^3)	V_b (cm^3)	t_x (min)	t_b (min)	f	Overall column capacity (mg)
20	20	5625	3895	1125	779	0.89	108.7
50	20	2700	1835	540	367	0.40	109.0
100	10	620	490	124	98	0.38	53.9
100	20	1360	675	272	135	0.61	109.3
100	30	1810	860	362	172	0.78	199.9

Flow rate: 5.0 cm^3 min^{-1}; f: fractional equilibrium capacity in the interaction region.

retention was investigated with laterite columns of different bed depths viz., 10, 20 and 30 cm. It is seen in Fig. 12b that as the bed height increase BTC becomes gentler. The breakthrough and exhaustion parameters are indicated in Table 3. Bed depth service time (BDST) model [39] that deals with the movement of an adsorption wave front through the adsorbent bed, expressed as:

$$t = \left[\frac{N}{C_0 F}\right] D - \left(\frac{1}{kC_0}\right) \ln\left[\frac{C_0}{C_t} - 1\right] \quad (12)$$

is tested. Here, N and k are the constants related to adsorption capacity and rate constant, respectively. A plot of service time (t (min)) against bed depth (D (cm)) yields a straight line (Fig. 13) with regression coefficient 0.9643. The column capacity at complete exhaustion was determined by taking the total area at the point where the effluent plot joins the exhaustion point of BTC and dividing the value by the weight of adsorbent in the column. It is found that the column capacity (per g of laterite) is approximately 1.2 times greater than the batch capacity.

3.7. Elution study

Elution becomes evident for the purpose of recovery of the retained metal ion in the column as well as the regeneration of the exhausted column bed for further use. Thermal regeneration in a multiple hearth furnace is the most common method used particularly for carbon column. However, in this approach, some adsorbent is lost during each cycle and recovery of the adsorbate is not possible. Chemical regeneration by a suitable solvent is a definite alternative. Almost quantitative recovery of Zn(II)

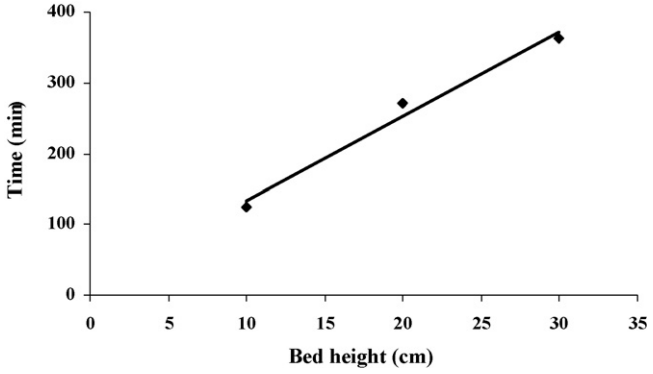

Fig. 13. Plot of BDST curve.

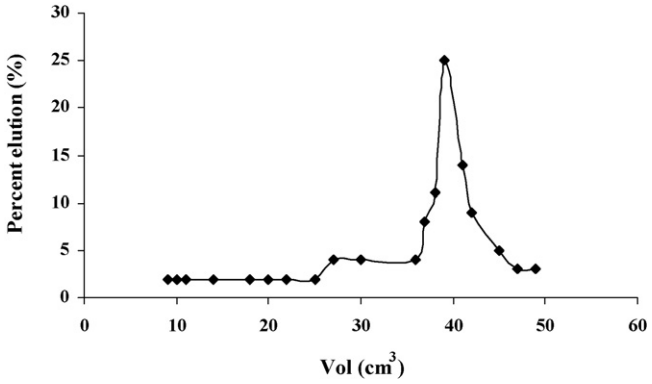

Fig. 14. Elution curve of retained zinc(II) from laterite column.

(80.5%) was observed with 1% HNO_3 (80 cm^3) as the eluting agent. The elution curve (Fig. 14) shows that the first 40 cm^3 of HNO_3 leads to 55.2% elution followed by elution of 25.3% with the rest 40 cm^3.

3.8. Column efficiency

In order to find out the adsorption efficiency of laterite column retention–elution cycles were repeated. The column was washed with 10 cm^3 fractions of distilled water at a fixed flow rate after the elution and was again fed with zinc solution. Fig. 15 represents the variation of column capacity as a function of operation number. It is found that, although, efficiency decreases with repetition of cycles, it remains within 85% even after eight cycles.

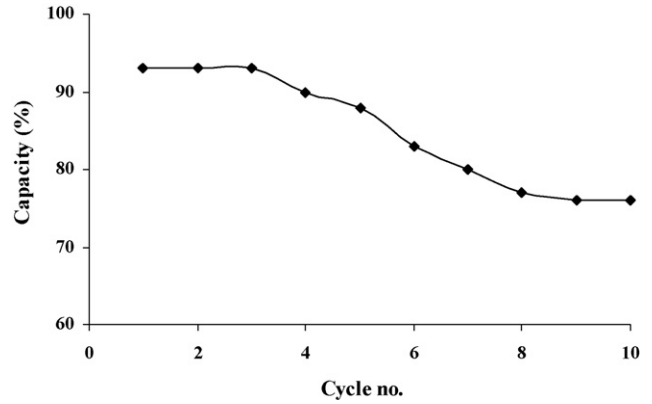

Fig. 15. Effect of cycle number on laterite column capacity for removal of zinc(II) from aqueous solution.

3.9. Cost estimation and relative efficiency of the process

The removal efficiency of metal ions [27] was calculated as:

$$\mathrm{RE} = \frac{C_0 - C_e}{C_0} \times 100 \quad (13)$$

where C_0 and C_e represent initial and equilibrium metal ion concentration, respectively. The removal efficiency of the laterite as well as cost of operation is compared with that of activated carbon (considered as a universal and most efficient adsorbent for treatment of metal bearing waste). The use of active carbon is limited due to its high cost. In several parts of India, laterite obtained as natural geomaterial is available in plenty and the estimated cost is approximately US \$25 tonne^{-1} (only transport cost is necessary) while that of the cheapest variety of commercially available carbon is approximately US \$285 tonne^{-1}. The Zn(II) adsorption capacity of laterite (5.57 mg g^{-1}) is found to be comparable to activated carbon as reported by Larsen and Schierup (6.2 mg g^{-1}) [40], more efficient than Filtrasorb-400 carbon (4.0 mg g^{-1}) but less efficient than Nuchar-SN carbon (66 mg g^{-1}) [41]. Thus, considering the removal efficiency laterite can be used as cost effective adsorbent for Zn(II) removal process and may be a good replacement for commercially available carbon.

4. Conclusion

Laterite, the naturally occurring geomaterial exhibits promising adsorption characteristics for the removal of Zn(II) and can be used as an alternative to active carbon, for the treatment of metal bearing wastewater. The process is feasible thermodynamically as indicated by negative free energy change and positive entropy change. The process is endothermic in nature and follows pseudo first order rate law. Freundlich adsorption isotherm is found to be fitted best. The column capacity is found to be higher than the batch capacity. The bed depth service time model is found to be applicable. Effective elution is made with 1% HNO_3 and 90% column efficiency is retained for six consecutive retention–elution cycles.

Acknowledgements

The authors are thankful to the authorities of Bhaba Atomic Research Centre, Mumbai, for the necessary permission and leave to Mr. J.L. Goswami. The authors also acknowledge the instrumental facilities provided by DST, Government of India, under FIST program.

References

[1] D.J. Horwarth, The Substances and Health—A Handbook, Marcel Dekker Inc., New York, 1996.
[2] World Health Organization, International Standards for Drinking Water, WHO, Geneva, 1971.
[3] M. Schlegel, A. Manceau, D. Chateigner, L. Charlet, Sorption of metal ions on clay minerals: I. Polarized EXAFS evidence for the adsorption of Co on the edges of hectorite particles, J. Colloid Interface Sci. 215 (1999) 140–158.
[4] M. Prasad, S. Saxena, S.S. Amritphale, N. Chandra, Kinetics and isotherms for aqueous lead adsorption by natural minerals, Ind. Eng. Chem. Res. 39 (2000) 3034–3037.
[5] M. Prasad, S. Saxena, S.S. Amritphale, Adsorption models for sorption of lead and zinc on francolite mineral, Ind. Eng. Chem. Res. 41 (2002) 105–111.
[6] S. Kaoser, S. Barrington, M. Elektorowicz, Li. Wang, Effect of Pb and Cd on Cu adsorption by sand–bentonite liners, Can. J. Civil Eng. 32 (2005) 241–249.
[7] V.K. Gupta, Equilibrium uptake, sorption dynamics, process development and column operations for the removal of copper and nickel from aqueous solution and wastewater using activated slag, a low-cost adsorbent, Ind. Eng. Chem. Res. 37 (1998) 192–202.
[8] J.M. Wang, X.J. Teng, H. Wang, H. Ban, Characterizing the metal adsorption capability of a class f coal fly ash, Environ. Sci. Technol. 38 (2004) 6710–6715.
[9] V.K. Gupta, M. Gupta, S. Sharma, Process development for the removal of lead and chromium from aqueous solutions using red mud—an aluminium industry waste, Water Res. 35 (2001) 1125–1133.
[10] A.H. Mahvi, D. Naghipour, F. Vaezi, S. Nazmara, Teawaste as an adsorbent for heavy metal removal from industrial wastewaters, Am. J. Appl. Sci. 2 (2005) 372–375.
[11] E.I. Shafey, M. Cox, A.A. Pichugin, Q. Appleton, Application of a carbon sorbent for the removal of cadmium and other heavy metal ions from aqueous solution, J. Chem. Technol. Biotechnol. 77 (2002) 429–436.
[12] Y. Guo, B. Din, Y. Liu, X. Chang, S. Meng, J. Liu, Preconcentration and determination of trace elements with 2-aminoacetylthiophenol functionalized amberlite XAD-2 by inductively coupled plasma-atomic emission spectrometry, Talanta 62 (2004) 209–215.
[13] M. Sarkar, P.K. Datta, M. Das, Solid phase extraction for the decontamination of alkali metal, alkaline earth metal and ammonium salts from heavy metal ions, J. Colloid Interface Sci. 246 (2002) 263–269.
[14] M. Sarkar, P.K. Datta, M. Das, Equilibrium studies on the optimization of solid phase extraction using modified silica gel for removal, recovery and enrichment prior to determination of some metal ions from aqueous samples of different origin, Ind. Eng. Chem. Res. 41 (2002) 6745–6750.
[15] K.Z. Perenyi, A. Laszicity, Z. Horvath, A. Levai, Use of a new type of 8-hydroxyquinoline-5-sulphonic acid cellulose (sulphoxime cellulose) for the preconcentration of trace metals from highly mineralised water prior their GFAAS determination, Talanta 47 (1998) 673–681.
[16] D. Prabhakaran, M.S. Subramanian, Enhanced metal extraction behavior using dual mechanism bifunctional polymer: an effective metal chelatogen, Talanta 61 (2003) 431–437.
[17] F. Bux, B. Atkinson, H.C. Kasan, Zinc Biosorption by waste activated and digested sludges, Water Sci. Technol. 39 (1999) 127–132.
[18] Y. Zhai, X. Wei, G. Zeng, D. Zhang, K. Chu, Study of adsorbent derived from sewage sludge for the removal of Cd^{2+}, Ni^{2+} in aqueous solutions, Sep. Purif. Technol. 38 (2004) 191–196.
[19] M. Zhao, J.R. Duncan, R.P. van Hille, Removal and Recovery of zinc from solution and electroplating effluent using *Azolla filiculoides*, Water Res. 33 (1999) 1516–1522.
[20] V.V. Basava Rao., S. Ram Mohan Rao, Biosorption isotherms of Pb (II) and Zn(II) on Pestan, an extracellular polysaccharide, of Pestalotiopsis sp. KCTC 8637P, Process Biochem. 41 (2006) 312–316.
[21] M. Vishwanadham, N. Sriramulu, A. Chary, Removal of Zn(II) and Ni(II) ions by using biopolymer chitin, Ind. J. Environ. Prot. 7 (2000) 515–521.
[22] M. Vithanage, R. Chandrajith, A. Bandara, R. Weerasooriya, Adsorption of zinc(II) from water with purified carbon nanotubes, Chem. Eng. Sci. 61 (2006) 1138–1145.
[23] S. Sen, K.G. Gupta, Bhattacharyya, Zn^{2+} and Sr^{2+} adsorption at the TiO_2 (110)–electrolyte interface: influence of ionic strength, coverage and anions, J. Colloid Interface Sci. 295 (2006) 50–64.
[24] S. Kundu, A.K. Gupta, Adsorption of some bivalent heavy metal ions from aqueous solutions by manganese nodule leached residues, J. Colloid Interface Sci. 293 (2006) 253–262.

[25] APHA, AWWA, WPCF, Standard Methods for the Examination of Water and Waste Water, nineteeth ed., Am. Wat. Works Assoc., New York, 1999.
[26] H.J. Fornwalt, R.A. Hutchins, Purifying liquids with activated carbon, Chem. Eng. 73 (1966) 179–183.
[27] M. Sarkar., A.R. Sarkar., J.L. Goswami, Removal of some toxic metal ions from water in a batch process using laterite, J. Ind. Chem. Soc., in press.
[28] D.F.S. Natusch, D.R. Taylor, Environmental effects of coal combustion, in: Chemical and Physical Characteristics of Coal Fly Ash, Part IV, Office of R&D, U.S., E.P.A., Minnesota, 1980.
[29] M. Sarkar, P.K. Datta, A.R. Sarkar, Sorption recovery of copper ion in aqueous solution using salicylaldoxime immobilsed silica gel, J. Ind. Pollut. Control 7 (2001) 179–190.
[30] S. Singh, A.K. Singh, G.S. Gupta, B.S. Tyagi, V.N. Singh, Adsorption of methylene blue from its aqueous solution by adsorption on fly ash, in: H.S. Ray, P.K. Jha (Eds.), Utilization of Natural Resources, Chemical Engineering Approach, Wiley Eastern Limited, New Delhi, India, 1984, pp. 194–201.
[31] A.K. Singh, D.P. Singh, V.N. Singh, Fly ash for the treatment of Zn(II) rich effluents, Environmentalist 11 (1991) 217–224.
[32] M. Sarkar, Use of fly ash for the removal of phenol and its analogues from contaminated water, Waste Manag. 26 (2006) 559–570.
[33] S. Qi, V.L. Snoeyink, W.E. Koffskey, B.W. Lykins, Using isotherms to predict GAC's capacity for synthetic organics, J. Am. Water Works Assoc. 84 (1992) 113–120.
[34] T.W. Weber, R.K. Chakraborty, Pore and solid diffusion models for fixed bed adsorbers, J. Am. Inst. Chem. Eng. 20 (1974) 228–238.
[35] N. Sakhayanwong, P. Thiraretyan, W. Nakleanpate, Adsorption mechanism of synthetic reactive dye wastewater by chitosan, J. Colloid Interface Sci. 286 (2005) 36–42.
[36] K. Periasamy, C. Namasivayam, Process development for the removal and recovery of cadmium from wastewater by a low cost adsorbent, Indust. Eng. Chem. Res. 33 (1994) 317–320.
[37] W.J. Weber, J.C. Morris, Kinetics of adsorption of carbon from solution, J. San. Eng. Div. 899 (1963) 31–39.
[38] M. Sarkar, A. Banerjee, P.P. Pramanick, Kinetics and mechanism of fluoride adsorption on laterite, Indust. Eng. Chem. Res. 45 (2006) 5920–5927.
[39] R.A. Hutchins, New method simplified design of activated carbon system, Chem. Eng. 80 (1973) 133–138.
[40] V.J. Larsen, H.H. Schierup, The Use of straw for removal of heavy metals from wastewater, J. Environ. Qual. 10 (1981) 188–194.
[41] C.H. Weng, C.P. Huang, Treatment of metal industrial wastewater by fly ash and cement fixation, J. Environ. Eng. Div. 120 (1994) 1470–1477.